Journal of Electroanalytical Chemistry 932 (2023) 117263

Contents lists available at ScienceDirect

Journal of Electroanalytical Chemistry

journal homepage: www.elsevier.com/locate/jelechem

Microelectrode-based probing of charge propagation and redox transitions in concentrated polyoxometallate electrolyte of potential utility for redox flow battery

Iwona A. Rutkowska [a,*], Anna Kesik [a], Claudia Janiszewska [a], Magdalena Skunik-Nuckowska [a], Krzysztof Miecznikowski [a], Lidia Adamczyk [b], Keti Vezzu [c], Enrico Negro [c], Vito Di Noto [c], Yongsheng Fu [d], Pawel J. Kulesza [a,*]

[a] Faculty of Chemistry, University of Warsaw, Pasteura 1, PL-02-093 Warsaw, Poland
[b] Czestochowa University of Technology, Faculty of Production Engineering and Materials Technology, Al. Armii Krajowej 19, 42-201 Czestochowa, Poland
[c] Department of Industrial Engineering, University of Padova, Via Marzolo 9, Padova, PD I-35131, Italy
[d] School of Chemistry and Chemical Engineering, Nanjing University of Science and Technology, Nanjing 210094, China

ARTICLE INFO

Dedicated to Professor Zbigniew Stojek on occasion of His 75th Birthday.

Keywords:
Redox electrolyte
Silicotungstic acid
Physical mass transport
Electron self-exchange hopping
Kinetic parameters
Microelectrode-based diagnosis

ABSTRACT

Concentrated solutions of Keggin-type silicotungstic acid, as well as the system's single crystals ($H_4SiW_{12}O_{40}$*$31H_2O$) and their colloidal suspensions have been tested using the microelectrode methodology to determine mass-transport, electron self-exchange and apparent (effective) diffusion-type coefficients for charge propagation and homogeneous (electron self-exchange) rates of electron transfers. Silicotungstic acid facilitates proton conductivity, and undergoes fast, reversible, multi-electron transfers leading to the formation of highly conducting, mixed-valence (tungsten(VI,V) heteropoly blue) compounds. To develop useful electroanalytical diagnostic criteria, electroanalytical approaches utilizing microdisk electrodes have been adapted to characterize redox transitions of the system and to determine kinetic parameters. Combination of microelectrode-based experiments performed in two distinct diffusional regimes: radial (long-term experiment; e.g., slow scan rate voltammetry or long-pulse chronoamperometry) and linear (short-term experiment; e.g., fast scan rate voltammetry or short-pulse chronocoulometry) permits absolute determination of such parameters as effective concentration of redox centers (C_o) and apparent transport (diffusion) coefficient (D_{app}). The knowledge of these parameters, in particular of $[D_{app}^{1/2} C_o]$ seems to be of importance to the evaluation of utility of redox electrolytes for charge storage. For the colloidal suspension of silicotungstic acid ($H_4SiW_{12}O_{40}$) crystals in the saturated solution, the following values have been obtained: D_{app} = 1.8*10^{-6} cm^2 s^{-1} and C_o = 1.1 mol dm^{-3}, as well as the $[D_{app}^{1/2} C_o]$ diagnostic parameter has reached the value as high as 6*10^{-3} mol/dm^{-3} cm s$^{-1/2}$, provided that four electrons are involved in the $H_4SiW_{12}O_{40}$ redox transitions. In this respect, the fact that crystals (dispersed solids) are characterized by high electron self-exchange rate (k_{ex} = 1.1*10^8 dm^3 mol^{-1} s^{-1}) and low activation energy (E_A = 18.7 kJ mol^{-1}) facilitating electron transfers between immobilized W^{VI} and W^{V} redox sites is also advantageous.

1. Introduction

Among stationary storage technologies, including grid-scale energy storage, which could be considered to overcome temporal deviations in energy production and consumption, redox flow batteries are important [1] thanks to their high power performance, flexible design, and ease of scaling-up. Flow batteries are rechargeable (secondary) cells, and they utilize one or more electroactive species dissolved in externally flowing electrolytes which are ready to accumulate all (or part) of the charge. The fundamental difference between conventional batteries and flow cells is that, in the previous case, energy is deposited the electrode material, whereas, in flow systems, it is accumulated in the redox electrolyte. Electrolytes are typically stored externally in tanks to be pumped through the cell but gravity-feed-type systems are also known. Recharging of flow batteries can be readily achieved

* Corresponding authors.
E-mail addresses: ilinek@chem.uw.edu.pl (I.A. Rutkowska), pkulesza@chem.uw.edu.pl (P.J. Kulesza).

https://doi.org/10.1016/j.jelechem.2023.117263
Received 30 November 2022; Received in revised form 3 February 2023; Accepted 8 February 2023
Available online 11 February 2023

by refilling tanks with the redox electrolyte, while the used material can be simultaneously recovered for future recharging.

The actual redox processes, which are responsible for the reversible conversion of chemical energy directly to electricity, occur at surfaces of the oppositely polarized electrodes, and they proceed within the redox electrolyte phases [2–4]. The present state of the art is represented by the all-vanadium redox flow batteries, even though they are still relatively expensive [5] and are characterized by a limited volumetric energy density. Many inorganic and organic electroactive systems have been proposed as alternatives [6–11] to the vanadium redox species for flow batteries. There is a need to search and characterize appropriate electroactive compounds that could function as robust reversible redox species in a rechargeable battery under flow conditions. In this respect, the appropriate methodology for preliminary testing and understanding of operation ought to be developed, as well as the relevant diagnostic criteria for evaluation of potential usefulness of redox electrolytes should be identified.

As the choice of redox-active charge-storage material has a significant impact on performance of the flow battery, care must be exercised to develop systems characterized by fast charge propagation and fast electron-transfers at the interfaces formed with electrode materials [12–18]. Provided that redox centers are fairly concentrated (certainly above 0.2 mol dm^{-3}), the electron self-exchange (hopping) mechanism should also be operative, in addition to physical mass transport (effectively diffusional or convective-diffusional), to influence the systems' current densities. The interplay between the kinetics of electron transfers and the viscosity-dependent mass transport dynamics would become even more important and affect over-all dynamics of electrochemical charging in highly concentrated solutions (greater than 2 mol dm^{-3}). Finally, to minimize ohmic drops, and to support unimpeded charge compensation, the redox electrolytes should be characterized by high ionic conductivity. Long-stability of components, including electrodes, is of importance as well.

From the viewpoint of potential applicability of concentrated solutions of redox electrolytes in flow batteries, the important parameters to be considered include physical diffusion (mass transport) coefficients, rates of electron transfers and electrochemical potentials at which reactions proceed [19–26]. For all-liquid systems, the mass transport parameter would play a crucial role in the electrochemical charging/discharging. Electron hopping (self-exchange), when is sufficiently high, may contribute to the overall charge propagation dynamics in redox electrolytes having electroactive species at concentrations higher than 0.2 mol dm^{-3}. Effectiveness of electron transfers would also be dependent on physicochemical parameters of redox molecules, such as ionic strength, total concentration, and viscosity.

To address the issues mentioned above, we consider a series of concentrated solutions of Keggin-type polyoxomettalate, silicododecatungstic acid ($H_4SiW_{12}O_{40}$) [26], as model redox electrolytes permitting fundamental considerations. To our best knowledge, this particular heteropolytungstic acid has so far been neither considered not fully characterized as redox system of potential importance to flow batteries. Polyoxometallates, are polynuclear inorganic materials with well-defined multi-electron reversible electrochemistry and electrocatalytic properties [27]. Among other important characteristics of heteropolyacids are that they exhibit very strong Brønsted acidity, act as proton conductors, and undergo fast, reversible, multi-electron transfers leading to the formation of highly conducting, mixed-valence tungsten(VI,V) heteropoly-blue centers [28]. Consequently, polyoxometallates are attractive components of redox catalysts or mediators in electrochemical processes [29–31].

To examine electrochemical properties and comment about potential utility of a redox electrolyte for the flow-battery-type systems, we explore here microelectrodes. Their use could lead to improvement in electrochemical data and should provide new diagnostic and analytical possibilities. Microelectrodes have been widely studied not only because of their compact size and utility in characterization of small samples but also because of such physical characteristics as the small electrode surface area and the related small double layer capacitance. Microelectrodes should be very useful in situations where macroelectrodes would give very large current densities in highly concentrated redox electrolytes. Indeed, small currents flowing through microelectrodes make ohmic drops negligible; consequently, the results obtained may be far more reliable and precise than those obtained with larger electrodes. Furthermore, because higher mas transport rates appear at microelectrodes, they should be useful in the study of electrode kinetics and chemical processes associated with charge-transfer step. Finally, electrochemical experiments utilizing microdisk electrodes should permit estimation of the effective diffusion coefficient and the concentration of redox sites in the concentrated redox electrolyte. This benefit arises because the electroanalytical experiment can be performed in two time regimes described in terms of two distinct mass-transfer patterns (linear and spherical) leading to two different equations that can be solved simultaneously for two unknowns, the concentration and the diffusion coefficient. The physicochemical meaning of these parameters, as well as the reliability of such determinations and their potential utility to other redox electrolytes will also be addressed here. In other words, we propose the unique microelectrode-based methodology permitting the preliminary examination of potential performance of highly concentrated redox solutions or suspensions.

2. Experimental

All chemicals were analytical grade materials and were used as received. Solutions were prepared from the deionized (Millipore Milli-Q) water. They were deoxygenated by bubbling with ultrahigh purified argon. Experiments were carried out at room temperature (22 ± 2 °C).

Chemical reagents were analytical grade materials. Silicotungstic acid hydrate was obtained from Sigma-Aldrich and sulfuric acid from POCh (Gliwice, Poland).

All electrochemical measurements were performed using a CH Instruments (Austin, TX, USA) Model 660 workstation in three electrodes configuration.

The microelectrode-based three-electrode cell (Fig. 1A) used for electrochemical investigations of concentrated redox electrolytes is analogous to that described earlier for solid-state voltammetry of "re-

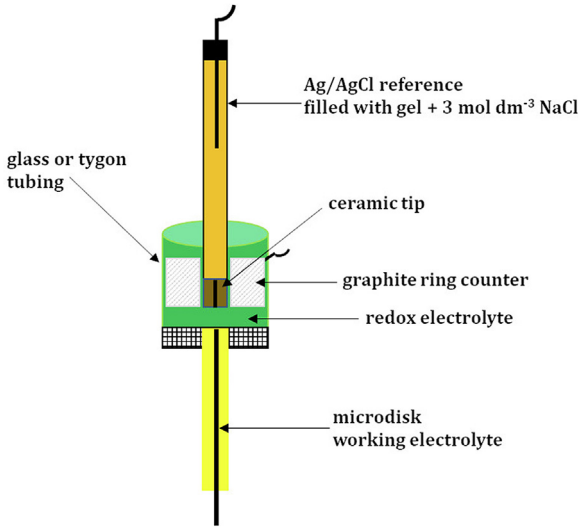

Fig. 1. (A) Schematic diagram of the microelectrode-based three-electrode electrochemical cell for characterization of redox electrolytes. (B) Cross-sectional view of the three-electrode assembly (utilizing microdisk working electrode and Ag/Ag_2O pseudoreference) for solid-state-type electrochemical experiments in absence of external liquid electrolyte.

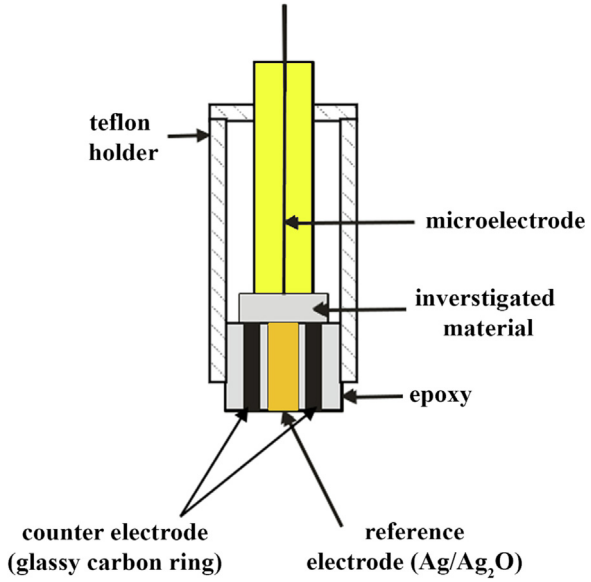

Fig. 1 (*continued*)

dox conducting" materials [26], except that solutions of silicotungstic acid ($H_4SiW_{12}O_{40}$), instead of electroactive crystals, have been introduced to the well-sealed cell chamber made up of a 10-μm diameter carbon fiber microdisk (Bioanalytical Systems) working electrode positioned opposite the gel-type reference electrode, which itself is surrounded by a relatively large graphite ring, as a counter electrode. The reference electrode (Bioanalytical Systems) was manufactured with a conducting gel (3 mol dm^{-3} NaCl/agar) electrolyte. A contact with the silicotungstic acid solution has been provided through the ion-permeable ceramic tip. This type of reference electrode works reproducibly and is virtually noncontaminating, and its small size simplifies construction of the measurement device. Furthermore, it acts as a potential standard, 0.20 V vs RHE. As a rule, between measurements, the reference electrode is stored in aqueous 3 mol dm^{-3} NaCl. For 30 min before each use, it is dipped into a gel prepared by heating 5 g of agar in 100 cm^3 of 3 mol dm^{-3} NaCl solution.

Comparative measurements with single crystals of silicotungstic acid ($H_4SiW_{12}O_{40}$*$31H_2O$) [26] have been performed using the three-electrode solid-state-type cell [32], in which the microdisk working electrode (10-μm diameter carbon fiber) is positioned opposite the planar probe comprising Ag/Ag_2O pseudoreference (~0.22 vs RHE), surrounded by glassy-carbon-ring counter electrode (Fig. 1B). Unless otherwise stated, all potentials reported here were recalculated and expressed vs the KCl-saturated Ag/AgCl (0.197 V vs RHE).

Single crystals of silicotungstic acid were grown at ambient temperature by slow evaporation of a saturated solution prepared by dissolution of 10 g of the commercially available 12-tungstosilicic acid (Sigma-Aldrich) in 5 cm^3 of Millipore deionized water. Typically crystals appeared after two days of growth.

Conventional cyclic voltammetric measurements were performed with use of a glassy carbon working electrode (geometric area, 0.071 cm^2). A glassy carbon rod and a KCl-saturated Ag/AgCl (Metroohm) served as counter and reference electrodes, respectively. The surface of glassy carbon was polished with aqueous alumina slurries on a Buehler polishing cloth and rinsed with distilled water.

3. Results and discussion

3.1. Silicotungstic acid concentrated solutions

The polyoxometallate-based redox electrolytes could be considered as anolytes or catholytes, depending on their redox potentials, but in many cases, their use would require formation of an asymmetric system with different-type redox species. Among representative systems, highly concentrated solutions of Keggin-type polyoxometallates of molybdenum ($H_4SiMo_{12}O_{40}$ or $H_3PMo_{12}O_{40}$) and tungsten ($H_4SiW_{12}O_{40}$ or $H_3PW_{12}O_{40}$) could serve as model examples of multi-electron systems for all-liquid redox flow batteries and related fundamental investigations. Among the polytungstates mentioned above, silicotungstic acid ($H_4SiW_{12}O_{40}$) is characterized by well-defined redox processes appearing at the relatively most negative potentials as well as by high over-all physicochemical stability. It is apparent from Fig. 2 that redox transitions (reversible reductions) characteristic of silicotungstic acid (Fig. 2A) start to appear at potentials almost 200 mV more negative relative to the analogous performance of phosphotungstic acid (Fig. 2B). The voltammetric peaks of silicotungstic acid (Fig. 2A) have height ratios 1:1:2, as expected from the literature [26] for Keggin-type heteropoly 12-tungstates. This behavior is consistent with the view that, depending on the applied potential, one, two, or four electrons are added and delocalized over the silicotungstate anion and, statistically, one, two, or four out of the 12 hexavalent tungsten atoms in the lattice are transformed into the pentavalent state, and the material becomes truly mixed-valence. The redox processes taking place in the polyanion are reversible and can generally be described as follows:

$$SiW_{12}O_{40}^{4-} + xe^- + xH^+ \leftrightarrow H_xSiW_{12}O_{40}^{4-} \quad (1)$$

where × can have values equal to 1, 2, and 4. It can be rationalized that the concentrated solutions of silicotungstic acid can be potentially used in a compartment of the negative electrode in a redox flow battery.

Microelectrodes are suitable for investigations of highly concentrated redox electrolytes where macroelectrodes would give very large current densities leading to significant ohmic drops. Electrochemical experiments utilizing microdisk electrodes permit estimation of the effective diffusion coefficient and the concentration of redox sites in the concentrated redox electrolyte. To perform diagnostic experiments and characterize concentrated silicotungstic acid solutions, we have utilized a measurement cell with a carbon fiber microdisk working electrode (Fig. 1A).

Results of the microelectrode based voltammetric measurements, which permit characterization of 0.6 mol dm^{-3} solution of the Keggin-type silicotungstic acid redox electrolyte, are illustrated in Figs. 3 and 4. The voltammetric experiments can be performed in two diffusional regimes: linear (Fig. 3) and radial (Fig. 4) executed at slow (5 mV s^{-1}) and fast (5 V s^{-1}) scan rates, respectively. Provided that the system is well-behaved (electrochemically reversible), a conventional Randles-Sevcik eqation is applicable under conditions of linear diffusion:

$$i_p = 2.69 * 10^5 n^{\frac{3}{2}} \pi r^2 D_{app}^{1/2} C_0 v^{1/2} \quad (2)$$

On the other hand, the steady state plateau currents can be described using a typical equation known for microdisk electrodes:

$$i_{ss} = 4nFD_{app}C_0 r \quad (3)$$

It is noteworthy that redox transitions of $H_4SiW_{12}O_{40}$ involve three consecutive fast and reversible redox processes involving one, one and two-electrons, respectively. The data implies not only the well-behaved character of the system but also permits absolute electroanalytical determination of the concentration of redox centers and effective (apparent) diffusion coefficient in a manner described earlier [18,26]. By combining two Eqs. (2) and (3), they can be resolved (see Eqs. (4) and (5) below for two unknowns: effective concentration of redox centers, C_0, and apparent (effective) diffusion (transport) coefficient, D_{app}.

$$C_0 = 4Fi_p^2/i_{ss}vn^2(2.69 * 10^5)^2\pi^2 r^3 \quad (4)$$

$$D_{app} = nv(2.69 * 10^5)^2\pi^2 r^2 i_{ss}^2/16F^2 i_p^2 \quad (5)$$

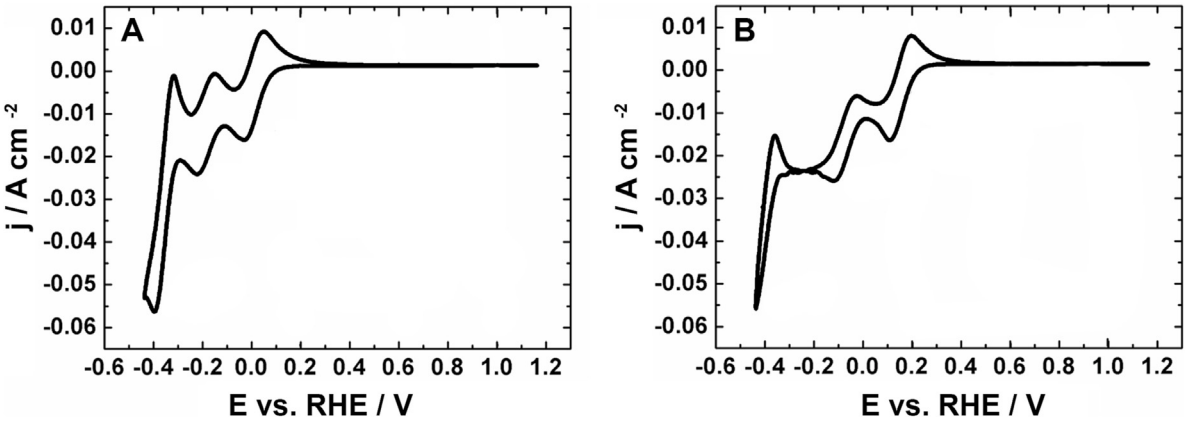

Fig. 2. Cyclic voltammetric responses recorded at 100 mV s^{-1} for (A) silicotungstic acid, and (B) phosphotungstic acid at 50 mmol dm^{-3} level. Working electrode: conventional glassy carbon (geometric surface area, 0.071 cm^2). The data are expressed vs the RHE reference electrode.

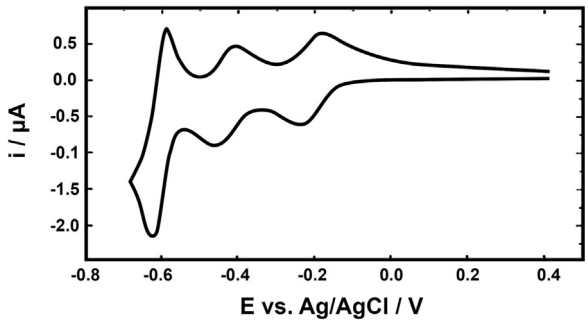

Fig. 3. Microelectrode-based voltammetry of 0.6 mol dm^{-3} silicotungstic acid redox electrolyte. Scan rate: 5 V s^{-1}. Reference electrode: Ag/AgCl gel-type system.

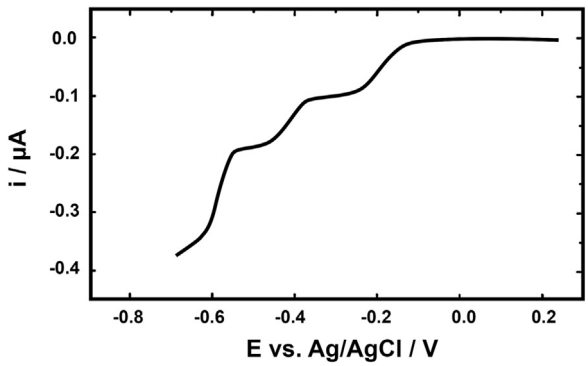

Fig. 4. Microelectrode-based voltammetry of 0.6 mol dm^{-3} solution of silicotungstic acid redox electrolyte. Scan rate: 5 mV s^{-1}. Reference electrode: Ag/AgCl gel-type system.

The analytical solution of these two equations results in C_0 = 0.59 (±0.01) mol dm^{-3} (which is not surprising and close to the nominal value of 0.6 mol dm^{-3}) and D_{app} = 1.2 (±0.01)*10^{-6} cm^2 s^{-1}. The latter value is consistent with the relatively fast transport coefficient characteristic of the 0.5 mol dm^{-3} $H_4SiW_{12}O_{40}$ solution. Here, the transport (diffusion) coefficient, D_{app}, can also be simply estimated using Eq. (3) from steady state current, i_{ss}, for the first (most positive) one-electron reduction plateau (Fig. 4) because the concentration (C_0) is known.

Using the simplified approach mentioned above, we have also observed that the D_{app}'s values tend to somewhat decrease upon increasing the concentration of $H_4SiW_{12}O_{40}$ (Fig. 5). It is reasonable to expect that viscosity becomes higher in more concentrated solutions and somewhat hinders the overall physical mass transport. On practical grounds, the effectiveness of the operation of redox electrolyte in battery type system will depend on both effective diffusion coefficient and the concentration of redox centers. It is noteworthy that current responses in such common electrochemical techniques as voltammetry (Eq. (2)) or chronoamperometry,

$$i = nFA[D_{app}{}^{1/2}C_0]/(\pi t)^{1/2} \quad (6)$$

are dependent on $[D_{app}^{1/2}\ C_0]$ parameter. For the series of concentrations, 0.1; 0.2; 0.4; 0.6; and 0.8 mol dm^{-3}, the $[D_{app}^{1/2}\ C_0]$ parameter becomes equal to 1.8*10^{-4}; 3.2*10^{-4}; 5.4*10^{-4}; 6.6*10^{-4}; and 7.0*10^{-4} mol dm^{-3} cm $s^{-1/2}$. The $[D_{app}^{1/2}\ C_0]$ parameter can be viewed as the measure of the effectiveness of charge propagation that is, obviously, crucial during the effective operation of battery type charge storage systems. It is apparent form the results calculated above for the series of silicotungstic acid concentrated solutions that the $[D_{app}^{1/2}\ C_0]$ parameter does not increase significantly at concentrations above 0.5 mol dm^{-3}. At higher concentrations, the mobility of ions, particularly of sizeable (ca. 1.2 nm [26]) heteropolytungstates, decreases due to increasing viscosity, and it starts to limit the physical mass transport. On the other hand, electron self-exchange (hopping) mechanism may become operative at higher concentrations to support the overall charge propagation.

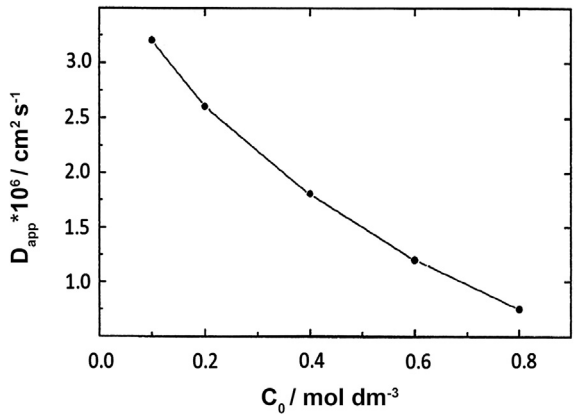

Fig. 5. Dependence of transport (diffusion) coefficient for charge propagation in redox electrolytes on concentration of $H_4SiW_{12}O_{40}$.

3.2. Mixed charge propagation mechanism: Fundamental considerations

The overall charge propagation process can be controlled by variety of phenomena such as physical mass transport, electron hopping rate, counterion displacement, coupling of physical diffusion and electron hopping [15,18]. Regardless the actual mechanism, the situation is advantageous when the overall rate of charge transport can be characterized in diffusional terms, i.e. using the apparent diffusion coefficient, D_{app}. In the case of solid-state-type systems, e.g. silicotungstic acid single crystals where the electron self-exchange rate, rather than the mobility of charge-compensation protons, is kinetically limiting factor, it is plausible to describe currents arising from electron hopping in term of a Fickian model with equivalent electron diffusion coefficient, D_e. Several theoretical treatments have related such a macroscopic property as D_e to site-to-site electron exchange rate constant (k_{ex});

$$D_e = \theta k_{ex} \delta^2 C_0 \quad (7)$$

where C_0 is the total concentration of redox sites, θ stands for a geometric factor that in the case of three-dimensional electron hopping becomes equal to 1/6, and δ is the distance between the redox sites at the time of electron transfer (that is usually estimated as the average intersite distance, $(C_0 N_A)^{-1/3}$, with N_A as Avogadro's number). It comes from Eq. (7) that both the population of the redox centers (C_0) and the rate constant for electron self-exchange (k_{ex}) must be large enough to develop a diffusion-controlled current. For concentrated redox electrolytes (between 0.5 and 4.5 mol dm^{-3}), the average site spacings (δ's) are from 0.4 to 1.8 nm. These facts can be kept in mind when redox systems are evaluated in terms of fast charge propagation.

The coupling of physical diffusion and electron self-exchange was initially developed to describe electron self-exchange reactions in solutions of redox ions [15,18]. The experimental diffusion rate, D_{app}, was found to be dependent on the physical diffusion rate, D_{phys}. When the k_{ex} electron self-exchange values are higher than 10^6 mol^{-1} dm^3 s^{-1}, they may contribute to the effective (apparent) charge transport coefficients [16]. Though separating electron and diffusion rates is not generally straightforward, useful information can be obtained from the so-called Dahms-Ruff relation, which in its corrected form [15,18] is as follows:

$$D_{app} = D_{phys} + D_e = D_{phys} + k_{ex} \delta^2 C_0 / 6 \quad (8)$$

To preserve electroneutrality, the electron transport (hopping or self-exchange) must be accompanied by the unimpeded motion of charge-compensating, structural, or interstitial counterions. Indeed, population of mobile protons in silicotungstic acid single crystal ($H_4SiW_{12}O_{40}$*$31H_2O$) is high, and their diffusive mobility does not limit electron transfers [26]. The ideal systems are the highly concentrated redox electrolytes in which D_{phys} and k_{ex} are maximized.

3.3. Electron self-exchange in $H_4SiW_{12}O_{40}$*$31H_2O$ single crystals

Single crystals of $H_4SiW_{12}O_{40}$*$31H_2O$ can be viewed as model systems with immobilized redox sites. The microelectrode-based solid-state electroanalysis of silicotungstic acid single crystals, which permitted the determination of the concentration of mixed-valence redox sites (that are electrochemically accessible in the system) and the effective diffusion coefficient for electron transfers (D_e), was described earlier [26]. It is noteworthy that silicotungstic acid single crystals are characterized by well-defined redox transitions appearing at potentials analogous to those characteristic of concentrated redox solutions. For simplicity and to avoid repetitions of the data published before [26], we provide here (*Supplementary material*) only voltammetric responses recorded at the microdisk electrode in two time regimes, related to the radial and linear diffusional charge propagation (Figs S1 and S2). The experiments have been performed here with use of a special measurement cell for solid-state voltammetry (Fig. 1A) which utilized the Ag/Ag_2O pseudoreference, rather than the gel-type reference Ag/AgCl system [26].

For the well-defined tetragonal $H_4SiW_{12}O_{40}$*$31H_2O$, the obtained values were as follows: C_0 = 1.5(±0.1) mol dm^{-3} or 1.5(±0.1)*10^{-3} mol cm^{-3}, and D_e = 2.8 ± 0.3*10^{-7} cm^2 s^{-1} where the error bars are standard deviations. The measurement approach was based on important characteristics of the potential step chronocoulometric and chronoamperometric experiments utilizing microdisk electrodes: the nature of mass transport depends on the time domain which in a case of the short-pulse experiment leads to the effectively linear flux of redox species perpendicular to the electrode, whereas spherical (non-linear) diffusion becomes predominant during the long-pulse experiment.

When using the above values of C_0 = 1.5*10^{-3} mol cm^{-3} and D_e = 2.8*10^{-7} cm^2 s^{-1} parameters, as well as by referring to Eq. (7) and to the already mentioned concept of the estimation of intersite distance (δ), we have estimated δ = 1.03*10^{-7} cm and k_{ex} = 1.1*10^8 dm^3 mol^{-1} s^{-1}. The latter electron self-exchange (k_{ex}) value is high, and it is approximately-two order of magnitude higher than that reported for the outer-sphere electron transfers in the model hexacyanoferrate(III, II) redox couple [16].

To get further insight into the nature and dynamics of electron transfers between W(VI) and W(V) in silicotungstic acid single crystals, we have determined D_e parameters at different temperatures 20, 15, 10, 5, and 0 °C (293, 288, 283, 278, and 273 K), respectively. Here the temperature ranges was restricted by the stability of $H_4SiW_{12}O_{40}$*$31H_2O$ single crystals. Provided that C_0 concentration is constant and equal to 1.5*10^{-3} mol cm^{-3}, the actual D_e values have been estimated from equation (7) upon consideration of the temperature-dependent steady-state current (i_{ss}) values characteristic of the first (most positive) one-electron plateau current (Fig. S1).

The Arrhenius-type logarithmic dependence of ln D_e on 1000/T [temperature T is in K] is shown in Fig. 6. Remembering that k_{ex} is strictly related to D_e, and by referring to the previous studies [33,34], the dependence can be understood as follows:

$$\ln k_{ex} = \ln k_{ex}^0 - E_A/RT \quad (9)$$

where k_{ex}^o stands for the electron self-exchange rate extrapolated toward infinitely high temperature and other parameters have usual significance. Here, the activation energy E_A can be determined from a slope of the dependence (Fig. 6). For the $H_4SiW_{12}O_{40}$*$31H_2O$ single crystal, the following values have been obtained: E_A = 18.7 kJ mol^{-1}, D_e^o = 6.1*10^{-4} cm^2 s^{-1} (i.e., D_e extrapolated to the infinitely high temperature), and k_{ex}^o = 2.3*10^{11} dm^3 mol^{-1} s^{-1}. On the basis of the results obtained, it can be concluded as follows. The linear dependence in Fig. 6 is consistent with the view that electron transfers within in H_4-

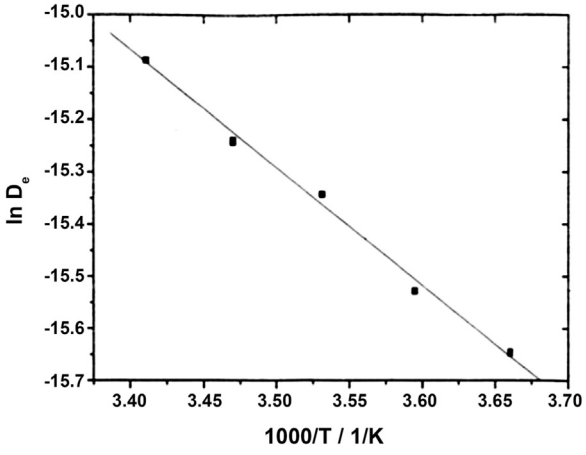

Fig. 6. The Arrhenius-type logarithmic dependence of ln D_e on *1000/T*.

$SiW_{12}O_{40}$*31H_2O single crystals with immobilized redox sites are thermally activated. Both the low value of the activation energy (E_A) and the high value of k^o_{ex} are consistent with the existence of very fast electron transfers between the immobilized redox sites in $H_4SiW_{12}O_{40}$*31-H_2O single crystals. In view of previous studies [16,33,34], the high value of k^o_{ex} parameter exceeding 10^{10} dm^3 mol^{-1} s^{-1} of the fast adiabatic process. Thus, it can be hypothesized that the electron self-exchange (hopping) mechanism can facilitate redox transitions in concentrated silicotungtic acid redox electrolytes.

3.4. Colloidal suspension of single crystals in concentrated solution

The 0.8 mol dm^{-3} silicotungstic acid solution is close to the level of saturation. To increase effectively the concentration of tungstate redox centers, we have considered the colloidal suspension of H_4SiW_{12}-O_{40}*31H_2O single crystals (5 g) dispersed (under magnetic stirring for 10 min) in 5 cm^3 of 0.8 mol dm^{-3} $H_4SiW_{12}O_{40}$ aqueous solution. It is apparent from Fig. 7 illustrating the system's cyclic voltammetric response recorded at the 10 V s^{-1} scan rate with use of the microdisk electrode (measurement cell of Fig. 1A) that the polytungstate redox transitions are still well-defined in the colloidal suspension of single crystals in concentrated solution despite application of high polarization rates leading to the linear diffusional patterns. We have also realized that application of microelectrodes produces – as in a case of single crystals [26] - concentration gradients that, upon application of a sufficiently short pulse (chronocoulometry) or a long pulse (chronoamperometry) either linear or spherical diffusional charge propagation is operative. To address calculations and interpretations, we performed the short-pulse (25 ms) and long-pulse (30 s) experiments in the chronocoulometric (Fig. 8) and chronoamperometric (Fig. 9) modes, respectively. In both cases, the step potential was to −0.440 V, i.e., to the potential that is approximately 80 mV more negative than the first reduction peak in Fig. 7.

Chronocoulometry gives the cumulative charge Q passed in reducing silicotungstatesites that are effectively transported to the microdisk electrode by linear diffusion along the concentration gradients developed within the colloidal suspension. As the experimental time scale increases, spherical diffusion predominates and a steady-state plateau currents are produced, as expected for chronoamperometry at microelectrodes [15–18,35,36]. As before [26], the approach has been based on the system of two equations describing two diffusional regimes: linear under chronocoulometric conditions,

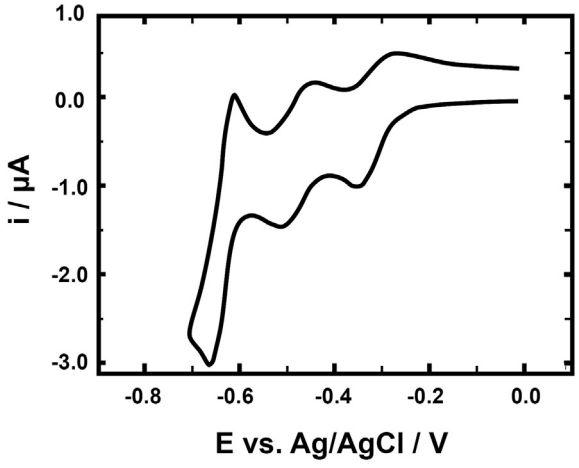

Fig. 7. Cyclic voltammetric response recorded at the 10 V s^{-1} scan rate (with use of the microdisk electrode) of the colloidal suspension of $H_4SiW_{12}O_{40}$*31-H_2O single crystals dispersed in 0.8 mol dm^{-3} $H_4SiW_{12}O_{40}$ aqueous solution. Reference electrode: Ag/AgCl gel-type system.

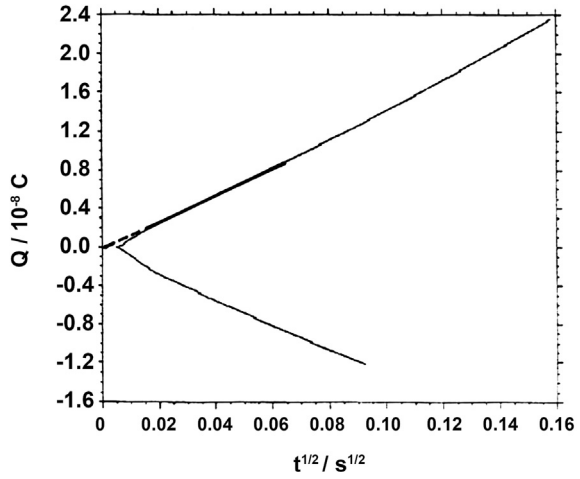

Fig. 8. Chronoculometric responses recorded using microdisk electrode of the colloidal suspension of $H_4SiW_{12}O_{40}$*31H_2O single crystals dispersed in 0.8 mol dm^{-3} $H_4SiW_{12}O_{40}$ aqueous solution. Short-pulse potential-step (25 ms) from 0.2 to −0.35 V. Reference electrode: Ag/AgCl gel-type system.

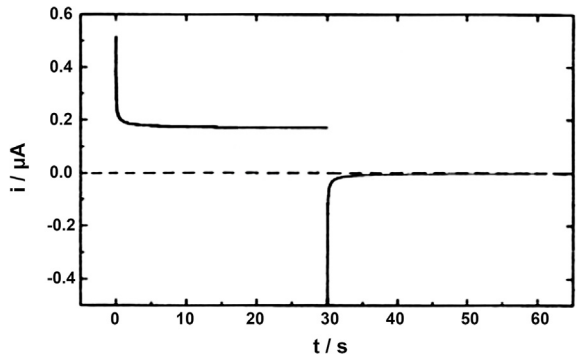

Fig. 9. Chronoamperometric responses recorded using microdisk electrode of the colloidal suspension of $H_4SiW_{12}O_{40}$*31H_2O single crystals dispersed in 0.8 mol dm^{-3} $H_4SiW_{12}O_{40}$ aqueous solution. Long-pulse potential-step (30 s) from 0.2 to −0.35 V. Reference electrode: Ag/AgCl gel-type system.

$$Q/t^{1/2} = 2nF\pi^{1/2}r^2C_0D_{app}^{1/2} \quad (10)$$

and radial using chronoamperometry (equation). They can be solved for two variables: C_o and D_e:

$$C_0 = \left(Q/t^{1/2}\right)^2/nF\pi r^3 i_{ss} \quad (11)$$

$$D_{app} = i_{ss}^2\pi r^2/4\left(Q/t^{1/2}\right)^2 \quad (12)$$

The dependency of Q versus $t^{1/2}$ (Anson plot) is shown in Fig. 8. As expected for a process controlled by linear diffusion, the plot is linear, and the slope is 119 (±2.2) nC s$^{-1/2}$. Further, the dependence showed effectively a zero intercept. The error bars are standard deviations based on the data from 10 independent experiments. The long-pulse chronoamperometry experiment (30 s pulse width) has featured a steady-state current response (Fig. 9), as expected from the predominantly nonlinear mass-transport mechanism. The response has been unchanged during at least 20 consecutive measurements. The mean value of the steady-state current, based on 10 independent experiments, has been equal to 183 ± 10nA. Finally, during the reverse pulse, the current decayed to zero, thus implying that the time scale of the measurement is long enough for the electrolysis products to diffuse away from the surface of the microdisk electrode.

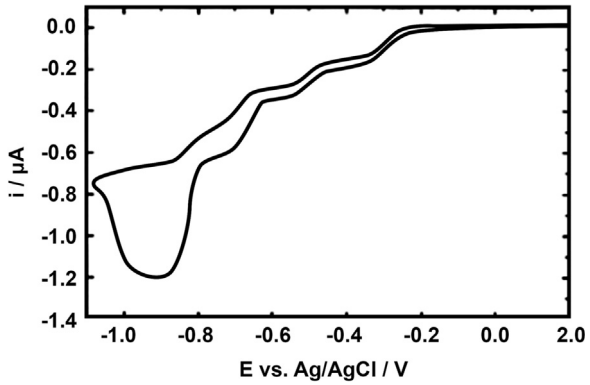

Fig. 10. Microelectrode-based voltammetry of the colloidal suspension of $H_4SiW_{12}O_{40}$*31H_2O single crystals dispersed in 0.8 mol dm^{-3} $H_4SiW_{12}O_{40}$ recorded in the extended potential range down to more negative potential values. Scan rate: 5 mV s^{-1}. Reference electrode: Ag/AgCl gel-type system.

Eqs. (11) and (12) yield D_{app} = 1.8(±0.3)*10^{-6} cm^2 s^{-1} and C_O = 1.1(±0.1) mol dm^{-3} where the error bars are standard deviations, as discussed above. The concentration of redox sites (C_O) is large enough to define the colloidal suspension as the over-saturated silicotungstic acid solution. The high value of D_{app} is consistent with the effectively fast diffusional charge propagation that may result from the possibility of mutual compensation between the physical mass transport and unimpeded electron hopping in the colloidal suspension of $H_4SiW_{12}O_{40}$. Thus the [$D_{app}^{1/2}$ C_O] parameter, which can be viewed as the measure of the effectiveness of charge propagation permitting effective charge storage, becomes fairly high and equals to 1.5*10^{-3} mol dm^{-3} cm $s^{-1/2}$. The present value has been estimated upon assumption that one electron is involved in the reduction of $H_4SiW_{12}O_{40}$. In reality, silicotungstates can accept reversibly up to 4 electrons during three reversible redox transitions and, under such conditions, the [$D_{app}^{1/2}$ C_O] parameter may reach the value of 6*10^{-3} mol dm^{-3} cm $s^{-1/2}$ which is close to the optimum values on the level of 10^{-2} mol dm^{-3} cm $s^{-1/2}$ characteristic of highly concentrated solutions (~10 mol dm^{-3}) characterized by high diffusion coefficients (larger than 10^{-6} cm^2 s^{-1}).

Finally, a microelectrode-based cyclic voltammetric experiment (Fig. 10) can provide useful information about applicable potential limits within which the colloidal suspension of $H_4SiW_{12}O_{40}$ can be practically considered as well-behaved redox electrolyte. In general, fundamental electrochemical studies are complicated in highly concentrated redox electrolytes in which population of supporting ions is comparable (rather than higher) to concentration of electroactive species. Although the migration effects also exist at microelectrodes [36], the problem is less severe upon application of microelectrodes [15–18]. It is apparent from Fig. 10 that, at potentials lower than ca. −0.65 V (i.e., following the first three well-known reversible silicotungstate redox transitions), the system is subject to irreversible reductions and possible reorganization [26]. Indeed, instead the well-defined plateau currents observed at microelectrodes at slow scan rates, the distorted waves and peaks are observed at potentials lower than −0.65 V. In other words, the present experiment implies that application of silicotungstic acid should be limited to the potentials not lower than −0.65 V.

4. Conclusions

Having in mind that current densities, which reflect dynamics of electrochemical processes, have an influence on the systems' performance, the viscosity of the electrolyte and the mass transport dynamics are also affected by the nature of the redox-active material and its concentration. Trying to develop useful electroanalytical diagnostic approaches, we have successfully utilized microelectrode-based probes, as well as the historical concepts of charge propagation in semi-solid or semi-liquid systems developed for mixed-valence polynuclear materials in order to characterize concentrated redox electrolytes. Among important parameters are concentration of redox centers (C_O) and apparent transport (diffusion) coefficient (D_{app}). The knowledge of these parameters and, in particular of [$D_{app}^{1/2}$ C_O], are crucial when it comes to evaluation of the diffusional-type charge propagation dynamics in the concentrated electrolyte which may reflect both physical mass transport and electron self-exchange (electron-hopping) contributions. Both potential-step (chronocoulometry, chronoamperometry) and cyclic voltammetric experiments utilizing microdisk electrodes have been adapted to characterization (identification of redox transitions and determination of kinetic parameters) of model inorganic redox electrolytes, namely highly-concentrated solutions or colloidal suspensions of Keggin-type polyoxometallates. For the colloidal suspension of silicotungstic acid ($H_4SiW_{12}O_{40}$) crystals in the saturated solution, the following values have been obtained: D_{app} = 1.8*10^{-6} cm^2 s^{-1} and C_O = 1.1 mol dm^{-3}, as well as the [$D_{app}^{1/2}$ C_O] diagnostic parameter has reached the value as high as 6*10^{-3} mol/dm^{-3} cm $s^{-1/2}$, provided that four electrons are involved in the $H_4SiW_{12}O_{40}$ redox transitions. In this respect, the fact that crystals (dispersed solids) are characterized by high electron self-exchange rate (k_{ex} = 1.1*10^8 dm^3 mol^{-1} s^{-1}) and low activation energy (E_A = 18.7-kJ mol^{-1}) facilitating electron transfers between immobilized W^{VI} and W^{V} redox sites is also advantageous. Our research parallel recent attempt to utilize the microelectrode-type systems to monitoring of charging/discharging processes and concentration changes during operation of redox flow batteries [37–39].

CRediT authorship contribution statement

Iwona A. Rutkowska: Conceptualization, Supervision, Methodology, Investigation, Formal analysis, Writing – original draft, Writing – review & editing. **Anna Kesik:** Investigation, Conceptualization, Data curation, Methodology. **Claudia Janiszewska:** Investigation, Data curation. **Magdalena Skunik-Nuckowska:** Investigation, Resources. **Krzysztof Miecznikowski:** Resources. **Lidia Adamczyk:** Resources. **Keti Vezzu:** Resources. **Enrico Negro:** Resources, Validation, Resources. **Vito Di Noto:** Validation, Resources, Supervision. **Yongsheng Fu:** Resources, Validation. **Pawel J. Kulesza:** Conceptualization, Methodology, Supervision, Formal analysis, Writing – original draft, Writing – review & editing.

Data availability

Data will be made available on request.

Declaration of Competing Interest

The authors declare that they have no known competing financial interests or personal relationships that could have appeared to influence the work reported in this paper.

Acknowledgements

This work was supported by National Science Center (NCN, Poland) under Opus Lap Project 2020/39/I/ST5/03385. Technical help of Michal P. Kulesza (Warsaw, Poland) is highly appreciated.

Appendix A. Supplementary data

Supplementary data to this article can be found online at https://doi.org/10.1016/j.jelechem.2023.117263.

References

[1] K. Lourenssen, J. Williams, F. Ahmadpour, R. Clemmer, S. Tasnim, Vanadium redox flow batteries: a comprehensive review, J. Energy Storage 25 (2019) 100844.

[2] Z. Yang, J. Zhang, M.C.W. Kintner-Meyer, X. Lu, D. Choi, J.P. Lemmon, J. Liu, Electrochemical Energy Storage for Green Grid, Chem. Rev. 111 (2011) 3577–3613.

[3] B. Dunn, H. Kamath, J.M. Tarascon, Electrical energy storage for the grid: a battery of choices, Science 334 (2011) 928–935.

[4] W. Wang, Q. Luo, B. Li, X. Wei, L. Li, Z. Yang, Recent progress in redox flow battery research and development, Adv. Funct. Mater. 23 (8) (2013) 970–986.

[5] O. Schmidt, S. Melchior, A. Hawkes, I. Staffell, Projecting the future levelized cost of electricity storage technologies, Joule 3 (1) (2019) 81–100.

[6] K. Gong, Q.R. Fang, S. Gu, S.F.Y. Li, Y.S. Yan, Nonaqueous redox-flow batteries: organic solvents, supporting electrolytes, and redox pairs, Energy Environ. Sci. 8 (2015) 3515–3530.

[7] T.B. Schon, B.T. McAllister, P.-F. Li, D.S. Seferos, The rise of organic electrode materials for energy storage, Chem. Soc. Rev. 45 (22) (2016) 6345–6404.

[8] L. Cheng, R.S. Assary, X. Qu, A. Jain, S.P. Ong, N.N. Rajput, K. Persson, L.A. Curtiss, Accelerating electrolyte discovery for energy storage with high-throughput screening, J. Phys. Chem. Lett. 6 (2) (2015) 283–291.

[9] S.D. Pineda Flores, G.C. Martin-Noble, R.L. Phillips, J. Schrier, Bio-inspired electroactive organic molecules for aqueous redox flow batteries. 1. Thiophenoquinones, J. Phys. Chem. C 119 (38) (2015) 21800–21809.

[10] Y. Moon, Y.-K. Han, Computational screening of organic molecules as redox active species in redox flow batteries, Curr. Appl. Phys. 16 (9) (2016) 939–943.

[11] P.J. Cappillino, H.D. Pratt, N.S. Hudak, N.C. Tomson, T.M. Anderson, M.R. Anstey, Application of redox non-innocent ligands to non-aqueous flow battery electrolytes, Adv. Energy Mater. 4 (2014) 1300566.

[12] J. Winsberg, T. Hagemann, T. Janoschka, M.D. Hager, U.S. Schubert, Redox-flow batteries: from metals to organic redox-active materials, Angew. Chem. Int. Ed. 56 (2017) 686–711.

[13] H. Chen, G. Cong, Y.-C. Lu, Recent progress in organic redox flow batteries: Active materials, electrolytes and membranes, J. Energy Chem. 27 (2018) 1304–1325.

[14] G. Inzelt, Mechanism of charge transport in polymer modified electrodes, in: A.J. Bard (Ed.), Electroanalytical Chemistry, vol. 18, Marcel Dekker, New York, 1994, pp. 89–241.

[15] N.A. Surridge, J.C. Jernigan, E.F. Dalton, R.P. Buck, M. Watanabe, H. Zhang, M. Pinkerton, T.T. Wooster, M.L. Longmire, J.S. Facci, R.W. Murray, The electrochemistry group medal lecture Electron self-exchange dynamics between redox sites in polymers, Faraday Discuss. 88 (1989) 1–17.

[16] P.J. Kulesza, E. Dickinson, M.E. Williams, S.M. Hendrickson, M.A. Malik, K. Miecznikowski, R.W. Murray, Electron self-exchange dynamics of hexacyanoferrate in redox polyether hybrid molten salts containing polyether-tailed counterions, J. Phys. Chem. B 105 (2001) 5833–5838.

[17] P.J. Kulesza, J.A. Cox, Solid-state voltammetry — Analytical prospects, Electroanalysis 10 (2) (1998) 73–80.

[18] P.J. Kulesza, M.A. Malik, Solid-state voltammetry, in: A. Wieckowski (Ed.), Interfacial Electrochemistry, Theory, Experiment and Applications, Marcel Dekker, New York, 1999, pp. 673–688.

[19] F. Andre, P. Hapiot, C. Lagrost, Phys. Chem. Chem. Phys. 12 (2010) 7506.

[20] O. Fontaine, C. Lagrost, J. Ghilane, P. Martin, G. Trippé, C. Fave, J.-C. Lacroix, P. Hapiot, H.N. Randriamahazaka, Mass transport and heterogeneous electron transfer of a ferrocene derivative in a room-temperature ionic liquid, J. Electroanal. Chem. 632 (1-2) (2009) 88–96.

[21] P. Hapiot, C. Lagrost, Electrochemical reactivity in room-temperature ionic liquids, Chem. Rev. 108 (7) (2008) 2238–2264.

[22] C. Lagrost, P. Hapiot, M. Vaultier, The influence of room-temperature ionic liquids on the stereoselectivity and kinetics of the electrochemical pinacol coupling of acetophenone, Green Chem. 7 (2005) 468–474.

[23] C. Lagrost, L. Preda, E. Volanschi, P. Hapiot, Heterogeneous electron-transfer kinetics of nitro compounds in room-temperature ionic liquids, J. Electroanal. Chem. 585 (1) (2005) 1–7.

[24] D. Zigah, J. Ghilane, C. Lagrost, P. Hapiot, Variations of diffusion coefficients of redox active molecules in room temperature ionic liquids upon electron transfer, J. Phys. Chem. B 112 (47) (2008) 14952–14958.

[25] D. Zigah, A. Wang, C. Lagrost, P. Hapiot, Diffusion of molecules in ionic liquids/organic solvent mixtures. Example of the reversible reduction of O_2 to superoxide, J. Phys. Chem. B 113 (7) (2009) 2019–2023.

[26] P.J. Kulesza, L.R. Faulkner, Solid-state electroanalysis of silicotungstic acid single crystals at an ultramicrodisk electrode, J. Am. Chem. Soc. 115 (25) (1993) 11878–11884.

[27] M. Sadakane, E. Steckhan, Electrochemical properties of polyoxometalates as electrocatalysts, Chem. Rev. 98 (1) (1998) 219–238.

[28] A.M. Herring, Inorganic-polymer composite membranes for proton exchange membrane fuel cells, Polym. Rev. 46 (2006) 245–296.

[29] A. Zurowski, A. Kolary-Zurowska, S. Dsoke, P.J. Barczuk, R. Marassi, P.J. Kulesza, Activation of carbon-supported platinum nanoparticles by zeolite-type cesium salts of polyoxometallates of molybdenum and tungsten towards more efficient electrocatalytic oxidation of methanol and ethanol, J. Electroanal. Chem. 649 (1-2) (2010) 238–247.

[30] J.B. Moffat, The surface and catalytic properties of heteropolyoxometalates, fundamental and applied catalysis, Kluwer Academic/Plenum Publishers, New York, 2001.

[31] P.J. Kulesza, K. Karnicka, K. Miecznikowski, M. Chojak, A. Kolary, P.J. Barczuk, G. Tsirlina, W. Czerwinski, Network electrocatalytic films of conducting polymer-linked polyoxometallate-stabilized platinum nanoparticles, Electrochim. Acta 50 (25-26) (2005) 5155–5162.

[32] A. Lewera, K. Miecznikowski, M. Chojak, O. Makowski, J. Golimowski, P.J. Kulesza, Iterative absolute electroanalytical approach to characterization of bulk redox conducting systems, Anal. Chem. 76 (10) (2004) 2694–2699.

[33] M.E. Williams, J.C. Crooker, R. Pyati, L.J. Lyons, R.W. Murray, A 10^{11}-fold range of solvent dynamics control of heterogeneous electron transfers of cobalt(III/II)tris (bipyridine), J. Am. Chem. Soc. 119 (42) (1997) 10249–10250.

[34] M.E. Williams, L.J. Lyons, J.W. Long, R.W. Murray, Transport and electron transfer dynamics in a polyether-tailed cobalt bipyridine molten salt: electrolyte effects, J. Phys. Chem. B 101 (1997) 7584–7591.

[35] Z. Stojek, J. Osteryoung, Experimental determination of the coefficient in the steady state current equation for spherical segment microelectrodes, Anal. Chem. 61 (11) (1989) 1305–1308.

[36] W. Hyk, Z. Stojek, Reverse pulse voltammetry and double potential step chronoamperometry as useful tools for characterization of electroactive systems under the conditions of mixed diffusional and migrational transport, Anal. Chem. 70 (1998) 5237–5243.

[37] B.J. Neyhouse, K.M. Tenny, Y.-M. Chiang, F.R. Brushett, A microelectrode-based sensor for measuring operando active species concentrations in redox flow cells, ACS Appl. Energy Mater. 4 (2021) 13830–13840.

[38] K. Zub, C. Stolze, P. Rohland, S. Stumpf, S. Hoeppener, M.D. Hager, U.S. Schubert, Inkjet-printed microband electrodes for a cost-efficient state-of-charge monitoring in redox flow batteries, Sens. Actuat. B Chem. 369 (2022) 132291.

[39] M. Wächtler, L. González, B. Dietzek, A. Turchanin, C. Roth, Functional materials: making the world go round, Phys. Chem. Chem. Phys. 21 (2019) 8988–8991.